JSEE Vol. 22, No. 2, 2020 DOI:10.48303/jsee.2020.246980

Research Note

This is an extended version of the paper presented in SEE8 conference, peer-reviewed again and approved by the JSEE editorial board.

Probabilistic Performance Appraisal of Seismic Structural Design Methodologies: A Case Study for RC/MRF Systems

Dariush Alimohammadi[1] and Esmaeel Izadi Zaman Abadi[2*]

1. M.Sc. Graduate, Department of Civil Engineering, Najafabad Branch, Islamic Azad University, Najafabad, Iran
2. Assistant Professor, Department of Civil Engineering, Najafabad Branch, Islamic Azad University, Najafabad, Iran, *Corresponding Author; email: e.izadi@pci.iaun.ac.ir

Received: 08/05/2020
Accepted: 01/09/2020

ABSTRACT

In this study, the effect of using two seismic design methodologies, Direct Displacement-Based Design (DDBD) and traditional Force-Based Design (FBD), on the probabilistic seismic performance of an 8-story RC moment resistant building is investigated. Also, two probabilistic procedures are applied for considering aleatory and epistemic uncertainties. Thus, this research is conducted by studying (i) non-linear static curve (ii) incremental dynamic analysis curve (iii) the Mean Annual Frequency (MAF) (iv) seismic demand of limit states (v) the confidence level of structures under the earthquakes with low to high hazard levels. Based on the comparing two mentioned seismic design methods, it can be said that the structure designed with FBD, unlike DDBD methodology is not capable of estimating performance goals. Also, it is concluded that the structure under both aleatory and epistemic uncertainties behaves more vulnerable and MAF of exceeding the immediate occupancy and collapse prevention is increased.

Keywords:
Direct displacement based design; RC frame; Nonlinear analysis; Probabilistic evaluation; Confidence level

1. Introduction

Direct Displacement-Based Design (DDBD) methodology is one of the performance-based seismic design methods, and with having a conceptual framework is suggested as an alternative design method for Force-Based Design (FBD). Priestley and Kowalsky [1] developed the details of DDBD procedure for RC frames. Pettinga and Priestley [2] investigated the dynamic behavior of six reinforced concrete frames using inelastic time history analyses. They suggested a new design displacement profile for DDBD procedure. Rahman and Sritharan [3] performed a comparative evaluation for the jointed wall systems designed with DDBD and FBD procedures. The results showed the satisfactory performance of DDBD procedure. Sullivan [4] applied DDBD methodology to a modern RC dual structural system. Malekpour et al. [5] discovered that steel frame structures have desirable performance even at taller models. Sullivan et al. [6] investigated the seismic performance of DDBD procedure for design of steel moment resistant frame structures. They showed that DDBD procedure can provide adequate control of seismic structural deformations. Wijesundara and Rajeev [7] developed the DDBD methodology for design of steel concentric braced structures. The results have a good agreement with the design considerations. Sullivan et al. [8] presented the software for DDBD method. Results showed that this software has excellent potential for using in the engineering profession. These researches led to publishing a

book by Priestley et al. [9] and model code DBD12 [10] for designing various structural systems. Nievas and Sullivan [11] achieved promising results by developing the DDBD design method for RC strong frame-weak wall structures with 4, 12, and 20 stories. Salawdeh and Goggins [12] found that DDBD method works relatively well on the design of single story steel concentrically braced structures and can predict base shear forces well. Peng and Guner [13] developed a new computer program to design RC frames based on direct displacement approach with the aiming facile design for engineers. Ye et al. [14] proposed DDBD methodology for designing base-isolated buildings. Performance comparison of 4 and 8 story RC structures designed with two DDBD and FBD methods by Sharma et al. [15] showed the high effectiveness of DDBD structures, unlike FBD. Senthilkumar and Satish Kumar [16] studied the seismic performance of composite frames with semi-rigid connections designed with DDBD approach. On the other hand, seismic performance evaluation of structures based on probabilistic principles due to the randomness of different structural parameters has recently been seriously considered. Among these probabilistic methods, the method proposed by Jalayer and Cornell [17] can be mentioned that is used as a criterion for estimating the reliability of structures.

In this study, probabilistic seismic performance of 8-story RC moment resistant building designed with DDBD and FBD methods are investigated and compared by studying (i) non-linear static curve (ii) incremental dynamic analysis curve (iii) the mean annual frequency (MAF) (iv) seismic demand of limit states (v) the confidence level of structures under the earthquakes with low to high hazard levels.

2. Direct Displacement-Based Design Brief

In Figure (1), basic steps of DDBD methodology

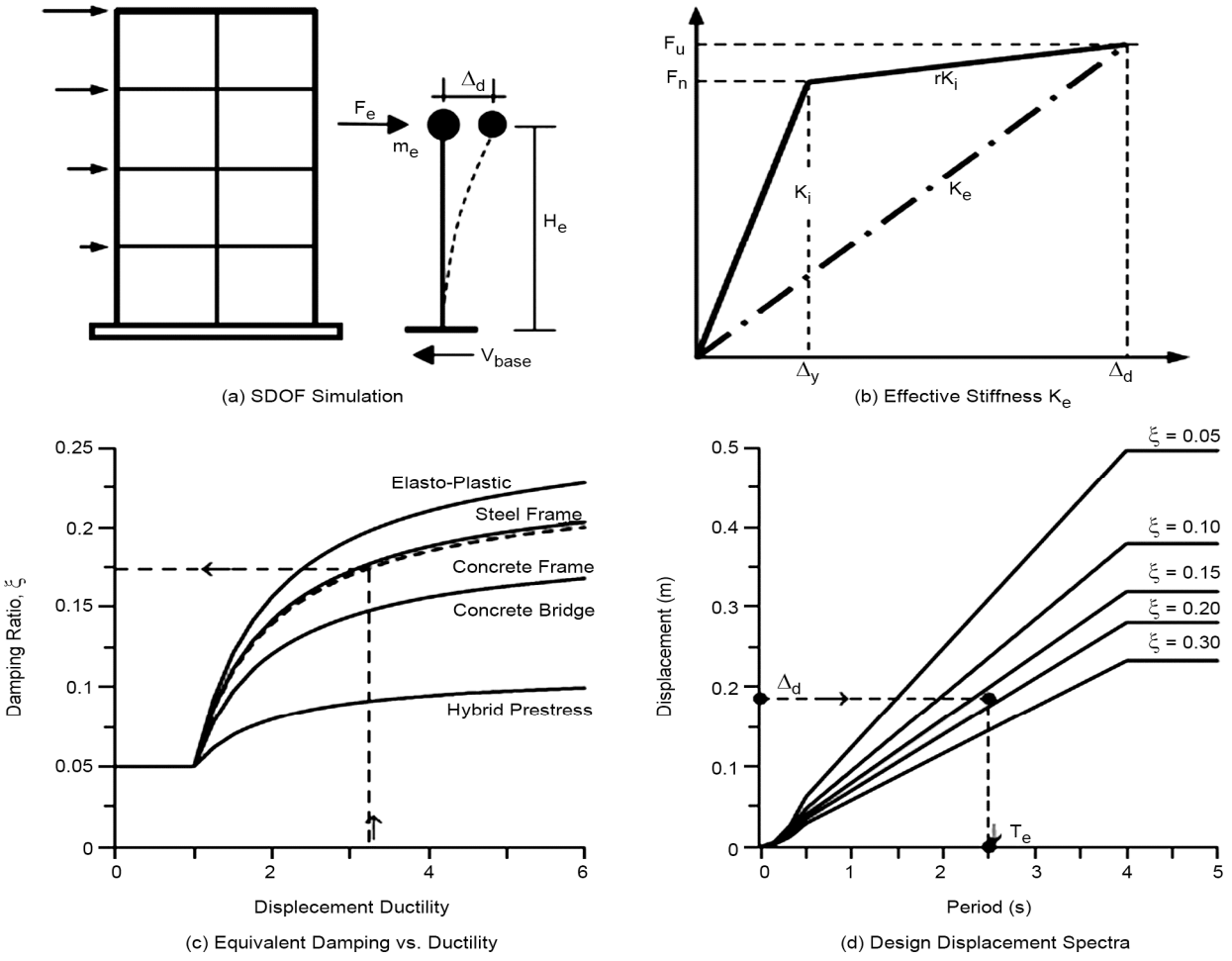

Figure 1. Conceptual framework of Direct Displacement-Based Design methodology [18].

(which is based on the substitute structure idea [19]) have been depicted. The basis of this design methodology is that it allows the designer to convert the Multi-Degree-Of-Freedom system (MDOF) into an equivalent Single-Degree-Of-Freedom system (e-SDOF). The properties of e-SDOF system are expressed by secant stiffness K_e at maximum design displacement Δ_d and a level of Equivalent Viscous Damping (EVD). For a certain amount of ductility and knowing frame type, EVD value is obtained from Figure (1c). In the following, the effective period T_e can be found for a known EVD value and the target displacement level (see Figure 1d). Figure (1d) depicts the reduced displacement spectrum that can be scaled for different damping levels. Finally, by calculating design base shear, the shear is distributed as equivalent lateral forces along the building height according to story masses. The full methodology may be found in [9] for RC frame buildings.

3. Case Study

An 8-story RC moment resistant frame building with typical plan and constant story height of 3 m is chosen as a case study (see Figure 2). The structure plan has three bays in each direction. The structural plan system is lateral load carrying. The inner bay length is 7 m and the length of outer bays is 4 m. In determining the dimensions and longitudinal reinforcement of beams and columns, the mean compressive strength of the concrete equal to 400 kg/cm^2 and the mean strength of reinforcing steel equal to 4000 kg/cm^2 was taken. The gravity load combination applied in the seismic analyses equal to $DL+0.2LL$ ($DL=800$ kg/m^2 and $LL=200$ kg/m^2) was considered. The building is assumed to be built in Tehran city with very high seismic hazard and soil type III specified by Iranian Earthquake Resistance Design Code [20]. To perform the non-linear analyses, the excitation is considered for X direction. The studied structure is designed in accordance with two DDBD and FBD methodologies in this article. In FBD methodology, the structure seismic design is done based on Iranian Earthquake Resistance Design Code for intermediate ductility class.

Calculations of bending moments and shear forces of beams and columns design for case study designed with DDBD methodology are reported in Tables (1) and (2). Design details of the case study building designed with two methodologies (DDBD based on the model code DBD12 provisions and FBD based on Iranian Earthquake Resistance Design Code provisions) are presented in Table (3). Note that in order to match the DDBD and FBD design methodologies, the design drift limit is considered to be 0.02 in the case study. This value is corresponding to repairable damage limit state in DDBD methodology and life safety limit state in FBD methodology.

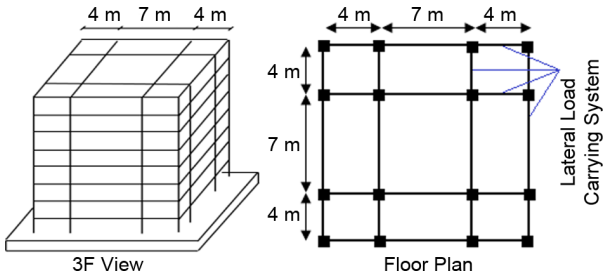

Figure 2. Schematic and plan view of the under-study building.

Table 1. Bending moments and shear forces of beams design for case study designed with DDBD method.

st	$M_{design,\ Outter\ span}$	$M_{design,\ Inner\ span}$	ϕ^0	External Frames		Internal Frames	
				$V_{design,\ Outter\ span}$	$V_{design,\ Inner\ span}$	$V_{design,\ Outter\ span}$	$V_{design,\ Inner\ span}$
8	139.6	145.3	1.25	110.6	93.8	125.7	141.7
7	218.7	229.1	1.25	166.7	125.6	181.5	173.2
6	290.9	304.7	1.25	216.8	154.3	231.7	201.9
5	348.5	367.4	1.25	260	178.8	274.7	226
4	394	418.1	1.25	295.8	199.1	310.3	245.9
3	433.1	459.7	1.25	323.8	215.1	338.2	261.9
2	460.1	488.3	1.25	343.1	226.1	357.5	272.9
1	474.1	503.1	1.25	353.1	231.8	367.5	278.6
							Units:kN, m

Note: In this table, *M* stands for moment, *V* for shear force, and ϕ^0 is overstrength factor.

Table 2. Bending moments and shear forces of columns design for case study designed with DDBD method.

st	μ	ϕ^0	ω_f	$M_{N1,\ Design}$ Exterior Column	$M_{N2,\ Design}$ Interior Column	ϕ_s	$V_{N1,\ Design}$ Exterior Column	$V_{N2,\ Design}$ Interior Column
8	1.03	1.25	1	169.94	339.88	0.75	163.29	326.58
7	1.17	1.25	1.09	183.28	366.56	0.75	246.98	493.96
6	1.47	1.25	1.17	263.17	526.35	0.75	326	651.99
5	1.47	1.25	1.17	319.72	639.44	0.75	387.49	774.97
4	1.47	1.25	1.17	366.63	733.26	0.75	438.5	877
3	1.47	1.25	1.17	403.07	806.14	0.75	478.13	956.26
2	1.47	1.25	1.17	428.2	856.4	0.75	505.46	1010.92
1	1.47	1.25	1.17	441.18	882.37	0.75	519.58	1039.16
								Units:kN, m

Note: In this table, *M* stands for moment, *N* for nominal, *V* for shear force, and μ, ϕ^0, ω_f, and ϕ_s are displacement ductility, overstrength factor, dynamic amplification factor for flexure, and strength reduction factor, respectively.

Table 3. Geometric dimension for prototype building designed with DDBD and FBD methods.

st	Column (Square)			Beam		Column (Square)	Beam	
	Corner Col.	Side Col.	Interior Col.	b_w	h_b		b_w	h_b
8	35	40	40	35	35	35	35	35
7	40	40	40	35	40	40	35	40
6	40	45	45	40	50	40	40	50
5	45	45	45	40	50	45	40	50
4	50	50	50	40	50	50	40	50
3	50	50	50	45	50	50	45	50
2	50	50	50	45	50	50	45	50
1	50	50	50	45	50	50	45	50
	DDBD Design Methodology					FBD Design Methodology		
	NB: b_w is the beam width; h_b is the total beam depth.					Unit: cm		

4. Analytical Modeling

Analytical model is developed in OpenSees framework. For this purpose, beams and columns are modeled using the nonlinear Beam Column element, and sections are considered as Fiber. The behavior model of materials for concrete and steel are concrete02 and steel02, respectively. Also to consider the confinement effect of transverse reinforcements, the parameters of confined concrete are calculated using Mander equations [21].

5. Verification of Modeling

In order to validate the numerical modeling technique used in this study, a two-story RC frame structure tested by Vecchio and Emara [22] is selected. The laboratory structure under-study has been tested using a quasi-static load and it is pushed until collapse occurred. Two constant vertical loads P = 700 kN have been applied at the top of the columns (see Figure 3). In the following, the tested frame geometry has been displayed in Figure 3). As shown in the figure, the frame has a single-span of 3.5 m and the story height of 2 m. The cross-section of columns and beams were reinforced with longitudinal rebars of diameter of 20 mm and stirrups with diameter of 10 mm at 125 mm spacing. The clear cover of beams and columns is 30 and 20 mm, respectively. The material properties i.e., concrete compressive strength, f_c^0, longitudinal rebar yield strength, f_y, and Young's modulus, E_s were considered 30, 418, and 192,500 MPa, respectively.

In Figure (4), the comparability of experimental results [22] with the analytical model developed in OpenSees and other studies results [23-25] has been demonstrated. There is a quite satisfactory agreement between the pushover analysis results of experimental and this study.

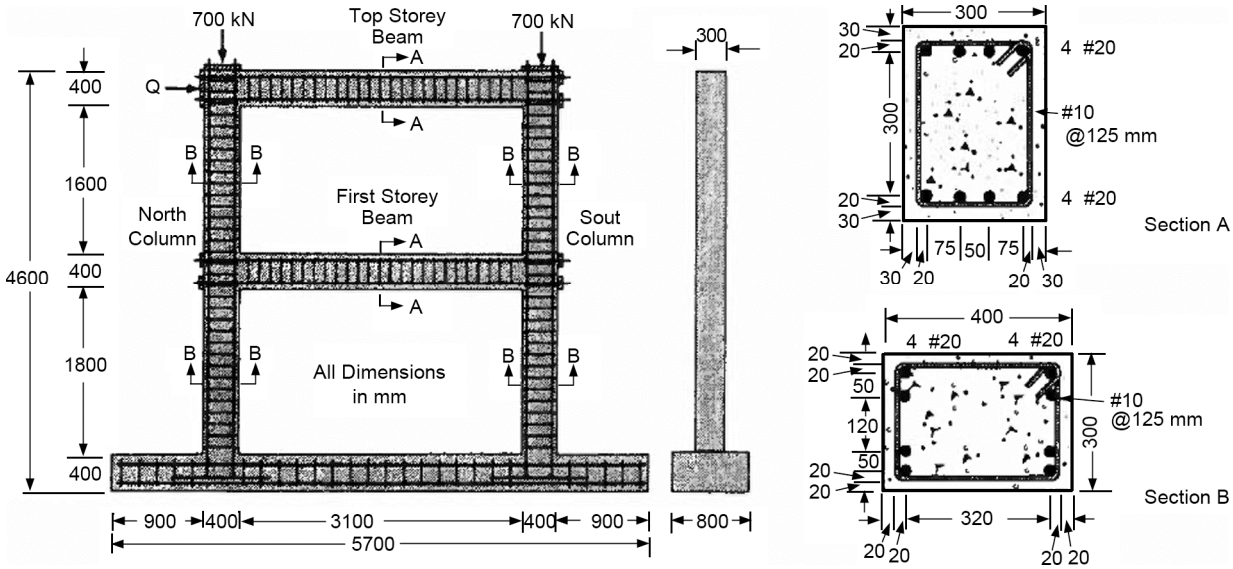

Figure 3. Details of large-scale RC frame tested by Vecchio and Emara [22].

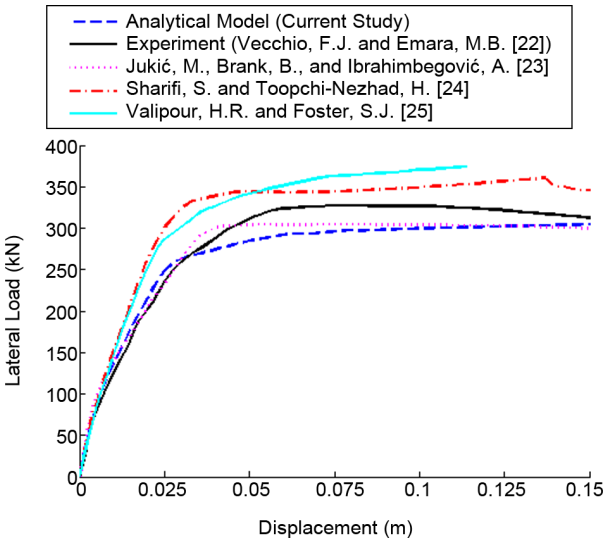

Figure 4. Comparing the results of numerical simulation with experiment.

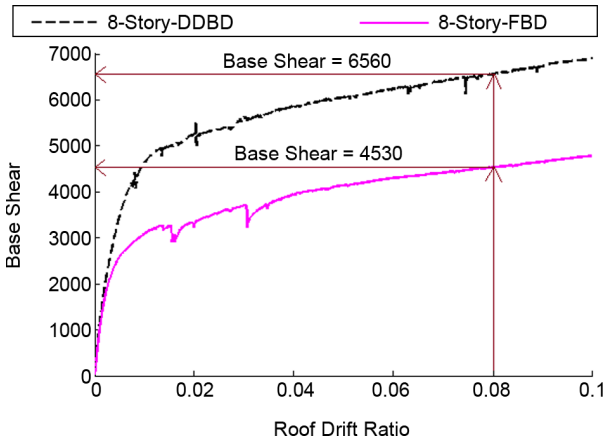

Figure 5. Comparing pushover curves of prototype building designed with DDBD and FBD methodologies.

6. Seismic Response

6.1. Nonlinear Static Analysis of Prototype Building

In the process of performing nonlinear static (pushover) analysis, the procedure presented in FEMA P695 [26] is used. According to provisions of these guidelines, the distribution of forces is performed in accordance with the structure's first-mode under the gravity load combination of 1.05DL + 0.25LL. In nonlinear static analyses, the analysis continues until the center of mass of the structure roof reaches a drift of 10%. In Figure (5), a comparison is made between the pushover curves of 8-story structure designed with two DDBD and FBD methodologies. As can be seen, in a certain amount of drift, e.g. drift of 8%, by changing the design methodology from DDBD to FBD, the base shear is reduced by 45%.

6.2. Nonlinear Dynamic Analysis of Prototype Building

In this article, the Incremental Dynamic Analysis (IDA) is employed to perform the reliability analysis of structures. Due to the dependence of the nonlinear behavior of structures to the earthquake record characteristics (eg frequency content), a set of earthquake records should be used to cover the entire range of structural behavior, i.e., linear to nonlinear.

Table (4) shows specifications of twenty far-field ground motions proposed by FEMA P695. All IDA analyses are done according to Hunt-Fill algorithm [27] and the results are plotted in IM-DM coordinate system. The considered IM (Intensity Measure) and DM (Demand Measure) indices in this study are maximum inter-story drift (θ_{max}) and 5%-damped first mode spectral acceleration ($S_a(T_1, 5\%)$), respectively. In the following, the definition of performance levels i.e., Immediate Occupancy (IO) and Collapse Prevention (CP) are performed according to FEMA-350 [28]. Based on FEMA-350, the IO performance level is defined for θ_{max} of 1.5%, and the CP performance level is defined for θ_{max} of 10% or 20% of the elastic slope. By deriving IDA curves, statistical fractiles are also obtained. There are two methods to draw 16%, 50% and 84% fractiles:

1. IM-based procedure: Based on this procedure, seismic responses (DM) are first sorted from small to large for the specific IM levels, then the numbers of 0.16 n_{rec}, 0.5 n_{rec}, and 0.84 n_{rec} (which for 20 ground motions is 3rd, 10th, and 16th number, respectively) are considered for 16, 50, and 84 percent fractiles, respectively. At low IM values, there is the DM value for all earthquake records, but with the increasing IM, since some records have reached the CP limit state, there is no DM value for those records. Thus, a big number indicating collapse must be considered for those records. Consequently, when seismic responses are sorted from small to large, those large numbers are placed at the bottom of the list. Note that in calculating the fractiles, instead of using the median numbers (i.e., 0.16 n_{rec}, 0.5 n_{rec}, and 0.84 n_{rec}), the mean numbers can also be used. However, because in higher earthquake intensities, a number of earthquake records collapse, calculation of mean numbers is faced with a problem.
2. DM-based procedure: In this procedure, at each level of the damage index (i.e., same DM), the IM values are sorted from small to large, and then the fractiles of 16, 50, and 84% are calculated. The disadvantage of the DM-based procedure is that since IDA curves of some earthquake records have successive segments of hardenings and softenings, there are several responses for an earthquake record at a specific DM level, and this issue makes it difficult to calculate 16, 50, and 84 percent fractiles.

Table 4. List of the considered earthquake records.

No.	Earthquake event	M_w	Station	NEHRP class	PGA/g
GM1	Chi-Chi, 1999	7.6	CHY101	D	0.44
GM2	San Fernando, , 1971	6.6	LA-Hollywood Stor	D	0.21
GM3	Friuli, 1976	6.5	Tolmezzo	C	0.35
GM4	Hector Mine, 1999	7.1	Hector	C	0.34
GM5	Kocaeli, 1999	7.5	Arcelik	C	0.22
GM6	Kocaeli, 1999	7.5	Duzce	D	0.36
GM7	Northridge, 1994	6.7	Canyon Country-WLC	D	0.48
GM8	Northridge, 1994	6.7	Beverly Hills - Mulhol	D	0.52
GM9	Imperial Valley, 1979	6.5	Delta	D	0.35
GM10	Imperial Valley, 1979	6.5	El CentroArray#11	D	0.38
GM11	Landers, 1992	7.3	Yermo Fire Station	D	0.24
GM12	Landers, 1992	7.3	Coolwater	D	0.42
GM13	Loma Prieta, 1989	6.9	Capitola	D	0.53
GM14	Loma Prieta, 1989	6.9	Gilroy Array #3	D	0.56
GM15	Superstition, 1987	6.5	H. El Centro Imp. Co.	D	0.36
GM16	Superstition, 1987	6.5	H. Poe Road (temp)	D	0.45
GM17	Kobe, 1995	6.9	Nishi-Akashi	C	0.51
GM18	Kobe, 1995	6.9	Shin-Osaka	D	0.24
GM19	Manjil, 1990	7.4	Abbar	C	0.51
GM20	Cape Mendo, 1992	7.0	Rio Dell Overpass	D	0.55

In this study, IM-based procedure to draw statistical fractiles has been used. In Figure (6), the IDA curves of the 8-story structure designed with two DDBD and FBD methodologies have been illustrated. As shown, in θmax of 0.06, IM value for 50th percentile (median) curve of the 8-story structure designed with DDBD methodology is reached to a value of 3 g and for the 8-story structure designed with FBD methodology is reached to a value of 1 g. Consequently, this significant reduction in the damage index indicates the inadequacy of FBD design methodology.

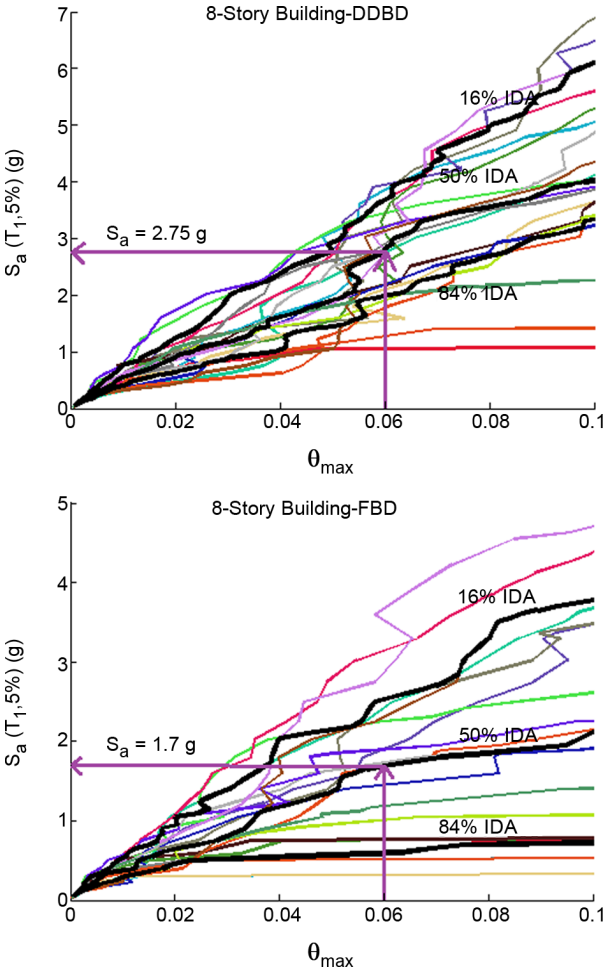

Figure 6. IDA curves of prototype building designed with DDBD and FBD methodologies.

7. Reliability Theory Formulation

In this study, the reliability assessment of structure designed with DDBD and FBD methodologies is performed with the aim of estimating confidence level and calculating MAF of exceedance. The following approximations [29] are used to calculate the MAF:

- It is assumed that the hazard curve can be expressed exponentially near the desired performance level in accordance with the following equation:

$$H(S_a) = k_0 S_a^{-k} \quad (1)$$

Parameters k and k_0 are coefficients for linear regression of hazard.

- It is assumed that the drift demand can be approximated by the following equation:

$$\hat{D} = a(S_a)^b \quad (2)$$

where a and b are regression coefficients for linear regression.

- It is assumed that the drift demand curve is log-normal and has a standard deviation equal to $\beta_{D/Sa}$ (dispersion factor).

7.1. Calculation of MAF

The MAF can be determined based on two evaluation procedures of "appraisal by considering the only source of uncertainty" and "appraisal by considering randomness and uncertainty as the sources of uncertainty" [17].

7.1.1. Appraisal by Considering the Only Source of Uncertainty

In calculating MAF, when only the aleatory uncertainty is contemplated for estimating the median of drift demand and drift capacity, the value of this parameter is obtained from Equation (3). Note that IDA analysis results are used to calculate drift demand median and drift capacity median.

$$P_{PL} = H(S_a^{\hat{c}}) \exp[\frac{1}{2}\frac{k^2}{b^2}(\beta_{D/S_a}^2 + \beta_C^2)] \quad (3)$$

where:

$$H(S_a^{\hat{c}}) = k_0 (S_a^{\hat{c}})^{-k} \quad (4)$$

in which, S_{ac} is the spectral acceleration of drift capacity level, $\beta_{D/Sa}$ is dispersion measure for drift demand and βc is dispersion measure for drift capacity.

7.1.2. Appraisal by Considering the Only Source of Uncertainty

In calculating MAF, when uncertainties of aleatory and epistemic are contemplated for estimating the median of drift demand and drift capacity, the value of this parameter is obtained from Equation (5):

$$P_{PL} = H(S_a^{\bar{c}}) \exp[\frac{1}{2}\frac{k^2}{b^2}(\beta_{D/S_a}^2 + \beta_{UD}^2)] \times \exp[\frac{1}{2}\frac{k^2}{b^2}(\beta_C^2 + \beta_{UC}^2)] \quad (5)$$

where:

$$H(S_a^{\bar{c}}) = k_0 (S_a^{\bar{c}})^{-k} . \exp(\frac{1}{2}\beta_{UH}^2) \quad (6)$$

$$\beta_{UD} = \frac{\beta_{D/S_a}}{\sqrt{n_{rec}}} \quad (7)$$

in which, β_{UD} is demand uncertainty, β_{UC} is capacity uncertainty and is assumed to be 0.2 for 8-story structure, β_{UH} is assumed to be 0.5 in this study, and n_{rec} is the number of earthquake records.

7.2. Calculation of Confidence Level

The calculating confidence level of structure is performed from:

$$CL = \varphi(K_x) \quad (8)$$

where:

$$K_x = -\frac{1}{\beta_{UT}} Ln(\frac{\gamma.D}{\varphi.C}) \quad (9)$$

in which, K_x is standardized Gaussian variate, β_{UT} is total uncertainty and for the case study building equal to 0.2 at IO performance level and equal to 0.425 at CP performance level is considered according to FEMA-350, and γ_D and ϕ_C are factored demand and factored capacity, respectively. The value of parameters of γ and ϕ can be calculated based on Equation (10) and Equation (11), respectively.

$$\gamma = \exp[\frac{1}{2}\frac{k}{b}\beta_{D/S_a}^2] \quad (10)$$

$$\varphi = \exp[-\frac{1}{2}\frac{k}{b}\beta_C^2] \quad (11)$$

8. Investigation of Results of Reliability Analysis

8.1. Investigation of Effect of Two Probabilistic Procedures on MAF Estimation

In Table (5), the MAF of exceeding the IO and CP performance levels has been illustrated. As seen, by changing the evaluation procedure from "appraisal by considering the only source of uncertainty" to "appraisal by considering randomness and uncertainty as the sources of uncertainty", the MAF value of exceeding the IO and CP performance levels for DDBD methodology is changed from 3.61×10^{-4} to 4.47×10^{-4} and 2.41×10^{-5} to 3.01×10^{-5}, respectively. Whereas for FBD methodology, it is changed from 6.35×10^{-4} to 7.7×10^{-4} and 5.58×10^{-4} to 6.89×10^{-4}, respectively. Hence, based on the results, it can be said that by considering aleatory and epistemic uncertainties, the MAF increases above 20 to 25 percent. Increasing this parameter increases the vulnerability of the structure. In comparing DDBD and FBD methodologies, the MAF value of exceeding the IO and CP performance levels under both aleatory and epistemic uncertainties for DDBD methodology are reached 3.61×10^{-4} and 2.41×10^{-5} and for FBD

Table 5. Comparing MAF of exceeding limit state by different probabilistic procedures.

	DDBD-The Only Source of Uncertainty		DDBD-Randomness and Uncertainty as the Sources of Uncertainty	
	IO	**CP**	**IO**	**CP**
MAF	3.61E-04	2.41E-05	4.47E-04	3.01E-05

	FBD-The Only Source of Uncertainty		FBD-Randomness and Uncertainty as the Sources of Uncertainty	
	IO	**CP**	**IO**	**CP**
MAF	6.35E-04	5.58E-04	7.70E-04	6.89E-04

methodology are reached 6.35×10^{-4} and 5.58×10^{-4}. As a result, it can be stated that by moving from FBD to DDBD methodology, MAF of exceeding the IO and CP performance levels decreases significantly.

8.2. Investigation of Confidence Level Changes vs. Drift Demand and Earthquake Intensity for Two DDBD and FBD Design Methodologies

The effect of seismic design methodologies on the structural confidence level has been investigated in Figure (7). A quick look at curves represented in Figure (7a) depicts that the structure designed with DDBD, unlike FBD methodology, up to the 4 g spectral acceleration satisfies 35% confidence level. In other words, FBD-designed structure at the spectral acceleration value of 2 g reaches to 0% confidence level. In the following, based on the mentioned figure, the spectral acceleration corresponding to 25, 50, 75, and 100% confidence levels for both DDBD and FBD methodologies can be derived. The results have been reported in Table (6). It is observed that the spectral acceleration at the 75% confidence level for DDBD-designed structure is 2.54 g whereas for FBD-designed structure is 0.52 g. Also, at 25% confidence level, the spectral acceleration value for the prototype structure designed with DDBD and FBD methodologies is equal to 4.53 and 0.88 g, respectively. Hence, it can be said that the spectral acceleration decreases dramatically by moving from the DDBD to FBD methodology for a specific value of confidence level. Finally, the decrease rate of structure confidence levels with demand increasing from 0 to 0.15 has been revealed in Figure (7b). In the structure designed with FBD methodology, the confidence level reaches zero at a demand value of 0.05. Whereas for the structure designed with DDBD methodology, a 79% confidence level is provided at the same value of demand and it is observed that the confidence level of 50% is still provided at the demand value of 0.071. This subject shows the great performance of DDBD methodology in the seismic design of structures.

8.3. Investigation of Effect of Using Two Design Methodologies in Distribution of Drift Demand and Confidence Level

In Figure (8a), the diagram of seismic demand changes under hazard levels of SLE25, SLE43, SLE72, DBE, MCE, and OVE has been displayed. By having seismic demand corresponding to hazard levels of low to high, confidence levels

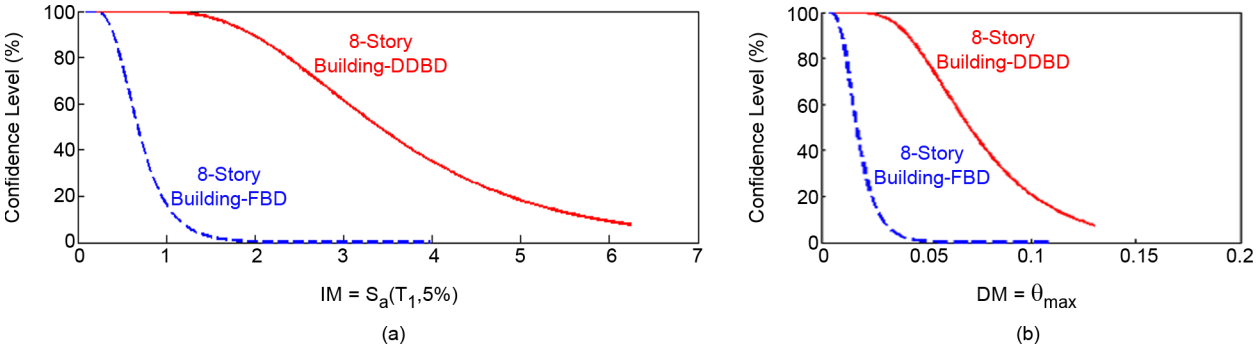

Figure 7. Curve of confidence level changes against a. seismic demand and b. seismic intensity.

Table 6. Calculation of spectral acceleration corresponding to 25, 50, 75, 100% confidence levels for DDBD and FBD methodology.

Spectral Acceleration Corresponding to a Confidence Level of 100%		Spectral Acceleration Corresponding to a Confidence Level Of 75%	
DDBD	**FBD**	**DDBD**	**FBD**
1.02 g	0.22 g	2.54 g	0.52 g
Spectral Acceleration Corresponding to a Confidence Level of 50%		**Spectral Acceleration Corresponding to a Confidence level of 25%**	
DDBD	**FBD**	**DDBD**	**FBD**
3.39 g	0.67 g	4.53 g	0.88 g

versus these hazard levels are obtained (see Figure 8b). These six hazard levels namely SLE25, SLE43, SLE72, DBE, MCE, and OVE have return periods of 25, 43, 72, 475, 2475, and 4975 years, respectively. As seen in Figure (8-a), by moving from the hazard level of SLE25 to OVE, the maximum demand value with a steep upward slope increases, and eventually, it reaches its maximum value at the OVE hazard level. For example, the maximum demand value at SLE25 hazard level corresponding to the CP performance level for the structure designed with DDBD methodology is equal to 0.0019, and it is reached to 0.025 for OVE hazard level corresponding to the CP performance level. Checking the confidence levels of structure designed with both DDBD and FBD methodologies at hazard levels of SLE25 to DBE corresponding to IO and CP performance levels (Figure 8-b) shows that it is reached to 95-99% because earthquakes with the return periods from 25 to 72 years are not among the strong earthquakes. Whereas at MCE and OVE hazard levels, the conditions for both mentioned design methodologies are quite different. For instance, at IO performance level corresponding to MCE and OVE hazard levels, DDBD-designed structure achieves 61 and 8% confidence level, respectively, and the confidence level of 99% is provided at CP performance level.

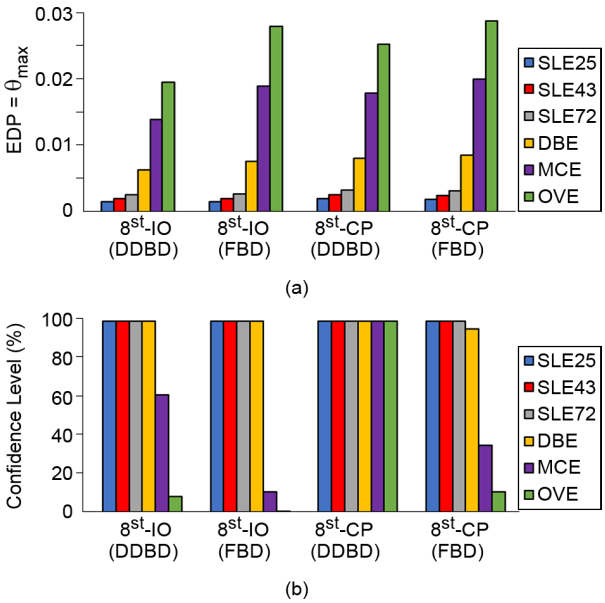

Figure 8. Distribution of (a) drift demand and (b) confidence level at different hazard levels for the DDBD and FBD methodologies.

However, by changing the design methodology from DDBD to FBD, the confidence levels versus MCE and OVE hazard levels at both IO and CP performance levels reduce. Hence, it can be said that reliability reduces dramatically by moving from DDBD to FBD.

9. Conclusion

Based on the probabilistic seismic performance appraisal of the 8-story RC frame building designed with DDBD and FBD methodologies, the following conclusions are obtained:

- The results of nonlinear evaluations showed that both pushover and IDA curves of structure designed with DDBD methodology, which derived from nonlinear analyses, are placed at a higher level than the curves of structure designed with FBD methodology. In other words, for a certain amount of roof drift, the base shear in the pushover curve of DDBD-designed structure increases dramatically compared to the pushover curve of FBD-designed structure. Besides, in IDA median curve, the earthquake intensity decreases dramatically for a certain amount of inter-story drift by moving from the DDBD to FBD methodology.
- In checking the vulnerability of the structure under study, it was concluded that by applying both aleatory and epistemic uncertainties, the MAF value of exceeding the immediate occupancy and collapse prevention increases in comparability to the state where only aleatory uncertainty is contemplated.
- The MAF value of exceedance considerably increases by changing the methodology from DDBD to FBD. The increasing this parameter indicates that the overall probability of failure in FBD-designed structure has increased.
- In investigating the confidence level changes versus intensity and demand, it was observed that by moving the design methodology from FBD to DDBD, the confidence level signify-cantly increases for a specific value of demand and intensity.
- By calculating the confidence level at different levels of seismic hazard, it was observed that

the structure designed with DDDB methodology, in contrast to FBD methodology is safe and provides the 99% confidence level at severe seismic hazard levels against the CP performance level.

References

1. Priestley, M.J.N. and Kowalsky, M.J. (2000) Direct displacement-based seismic design of concrete buildings. *Bulletin of the New Zealand Society for Earthquake Engineering*, **33**(4), 421-441.

2. Pettinga, J.D. and Priestley, M.J.N. (2005) Dynamic behaviour of reinforced concrete frames designed with direct displacement-based design. *Journal of Earthquake Engineering*, **9**(SPEC. ISS. 2), 309-330.

3. Rahman, M.A. and Sritharan, S. (2006) An evaluation of force-based design vs. direct displacement-based design of jointed precast post-tensioned wall systems. *Earthquake Engineering and Engineering Vibration*, **5**(2), 285-296.

4. Sullivan, T.J. (2011) Direct displacement-based design of a RC wall-steel EBF dual system with added dampers. *Bulletin of the New Zealand Society for Earthquake Engineering*, **44**(3), 167-178.

5. Malekpour, S., Ghaffarzadeh, H., and Dashti, F. (2011) Direct displacement based design of regular steel moment resisting frames. *Procedia Engineering*, **14**, 3354-3361.

6. Sullivan, T., Maley, T., and Calvi, G.M. (2011) Seismic response of steel moment resisting frames designed using a Direct DBD procedure. *Proceedings of the 8th International Conference on Structural Dynamics, EURODYN.*

7. Wijesundara, K. and Rajeev, P. (2012) Direct displacement-based seismic design of steel concentric braced frame structures. *Australian Journal of Structural Engineering*, **13**(3),243-257.

8. Sullivan, T.J., Bono, F., Magni, F., and Calvi, G.M. (2012) Development of a computer program for direct displacement-based design. *15th World Conference Earthquake Engineering.*

9. Priestley, M.J.N., Calvi, G.M., and Kowalsky, M. (2007) *Displacement-Based Seismic Damage of Structures*. Pavia, Italy: IUSS Press.

10. Sullivan, T.J., Priestley, M.J.N., and Calvi, G.M. (2012) *A Model Code for the Displacement-Based Seismic Design of Structures DBD12.*

11. Nievas, C.I. and Sullivan, T.J. (2014) Developing the direct displacement-based design method for RC strong frame-weak wall structures. *Second European Conference on Earthquake Engineering and Seismology*, Instanbul 25-29.

12. Salawdeh, S. and Goggins, J. (2016) Direct displacement based seismic design for single storey steel concentrically braced frames. *Earthquake and Structures*, **10**(5), 1125-1141.

13. Peng, C. and Guner, S. (2018) Direct displacement-based seismic assessment of concrete frames. *Computers and Concrete*, **21**(4), 355-365.

14. Ye, K., Xiao, Y., and Hu, L. (2019) A direct displacement-based design procedure for base-isolated building structures with lead rubber bearings (LRBs). *Engineering Structures*, **197**, 109402.

15. Sharma, A., Tripathi, R.K., and Bhat, G. (2020) Comparative performance evaluation of RC frame structures using direct displacement-based design method and force-based design method. *Asian Journal of Civil Engineering*, **21**(3), 381-394.

16. Senthilkumar, R. and Satish Kumar, S.R. (2020) Seismic performance of semi-rigid steel-concrete composite frames. *Structures*, **24**, 526-541.

17. Jalayer, F. and Cornell, C.A. (2003) *A Technical Framework for Probability-Based*

Demand and Capacity Factor Design (DCFD) Seismic Formats. Report No. 2003/08, Pacific Earthquake Engineering Center, Berkeley, CA.

18. Priestley, M.J.N., Calvi, G.M., and Kowalsky, M.J. (2007) Direct displacement-based seismic design of structures. *NZSEE Conference*

19. Shibata, A. and Sozen, M.A. (1976) Substitute-structure method for seismic design in R/C. *Journal of the Structural Division*, **102**(1), 1-18.

20. Standard No. 2800 (2015) *4th Edition of Iranian Code of Practice for Seismic Resistance Design of Buildings*. Building and Housing Research Center, Iran (in Persian).

21. Mander, J.B., Priestley, M.J.N., and Park, R. (1988) Theoretical stress-strain model for confined concrete. *Journal of Structural Engineering*, **114**(8), 1804-1826.

22. Vecchio, F.J. and Emara, M.B. (1992) Shear deformations in reinforced concrete frames. *ACI Structural Journal*, **89**(1), 46-56.

23. Jukić, M., Brank, B., and Ibrahimbegović, A. (2013) Embedded discontinuity finite element formulation for failure analysis of planar reinforced concrete beams and frames. *Engineering Structures*, **50**, 115-125.

24. Sharifi, S. and Toopchi-Nezhad, H. (2018) Seismic response modification factor of RC-frame structures based on limit state design. *International Journal of Civil Engineering*, **16**(9), 1185-1200.

25. Valipour, H.R. and Foster, S.J. (2010) A total secant flexibility-based formulation for frame elements with physical and geometrical nonlinearities. *Finite Elements in Analysis and Design*, **46**(3), 288-297.

26. Federal Emergency Management Agency (2009) *Quantification of Building Seismic Performance Factors*. Washington, DC: FEMA P695.

27. Vamvatsikos, D. (2011) Performing incremental dynamic analysis in parallel. *Computers and Structures*, **89**(1-2), 170-180.

28. Federal Emergency Management Agency (2000) *Recommended Seismic Design Criteria for New Steel Moment-Frame Buildings*. Washington, D.C: FEMA-350.

29. Cornell, C.A., Jalayer, F., Hamburger, R.O., and Foutch, D.A. (2002) Probabilistic basis for 2000 SAC federal emergency management agency steel moment frame guidelines. *Journal of Structural Engineering*, **128**(4), 526-533.

book by Priestley et al. [9] and model code DBD12 [10] for designing various structural systems. Nievas and Sullivan [11] achieved promising results by developing the DDBD design method for RC strong frame-weak wall structures with 4, 12, and 20 stories. Salawdeh and Goggins [12] found that DDBD method works relatively well on the design of single story steel concentrically braced structures and can predict base shear forces well. Peng and Guner [13] developed a new computer program to design RC frames based on direct displacement approach with the aiming facile design for engineers. Ye et al. [14] proposed DDBD methodology for designing base-isolated buildings. Performance comparison of 4 and 8 story RC structures designed with two DDBD and FBD methods by Sharma et al. [15] showed the high effectiveness of DDBD structures, unlike FBD. Senthilkumar and Satish Kumar [16] studied the seismic performance of composite frames with semi-rigid connections designed with DDBD approach. On the other hand, seismic performance evaluation of structures based on probabilistic principles due to the randomness of different structural parameters has recently been seriously considered. Among these probabilistic methods, the method proposed by Jalayer and Cornell [17] can be mentioned that is used as a criterion for estimating the reliability of structures.

In this study, probabilistic seismic performance of 8-story RC moment resistant building designed with DDBD and FBD methods are investigated and compared by studying (i) non-linear static curve (ii) incremental dynamic analysis curve (iii) the mean annual frequency (MAF) (iv) seismic demand of limit states (v) the confidence level of structures under the earthquakes with low to high hazard levels.

2. Direct Displacement-Based Design Brief

In Figure (1), basic steps of DDBD methodology

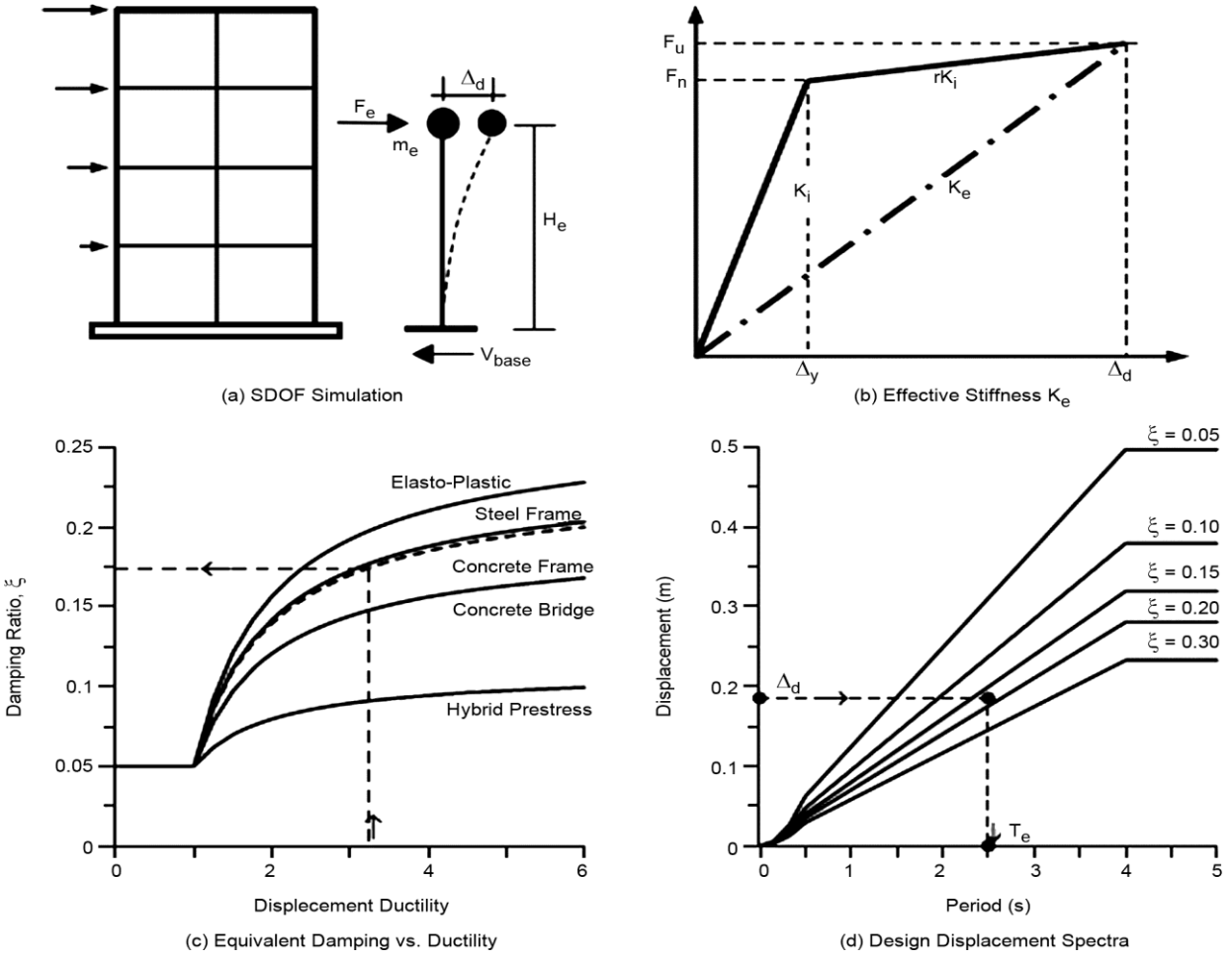

Figure 1. Conceptual framework of Direct Displacement-Based Design methodology [18].

(which is based on the substitute structure idea [19]) have been depicted. The basis of this design methodology is that it allows the designer to convert the Multi-Degree-Of-Freedom system (MDOF) into an equivalent Single-Degree-Of-Freedom system (e-SDOF). The properties of e-SDOF system are expressed by secant stiffness K_e at maximum design displacement Δ_d and a level of Equivalent Viscous Damping (EVD). For a certain amount of ductility and knowing frame type, EVD value is obtained from Figure (1c). In the following, the effective period T_e can be found for a known EVD value and the target displacement level (see Figure 1d). Figure (1d) depicts the reduced displacement spectrum that can be scaled for different damping levels. Finally, by calculating design base shear, the shear is distributed as equivalent lateral forces along the building height according to story masses. The full methodology may be found in [9] for RC frame buildings.

3. Case Study

An 8-story RC moment resistant frame building with typical plan and constant story height of 3 m is chosen as a case study (see Figure 2). The structure plan has three bays in each direction. The structural plan system is lateral load carrying. The inner bay length is 7 m and the length of outer bays is 4 m. In determining the dimensions and longitudinal reinforcement of beams and columns, the mean compressive strength of the concrete equal to 400 kg/cm^2 and the mean strength of reinforcing steel equal to 4000 kg/cm^2 was taken. The gravity load combination applied in the seismic analyses equal to $DL + 0.2LL$ ($DL = 800$ kg/m^2 and $LL = 200$ kg/m^2) was considered. The building is assumed to be built in Tehran city with very high seismic hazard and soil type III specified by Iranian Earthquake Resistance Design Code [20]. To perform the non-linear analyses, the excitation is considered for X direction. The studied structure is designed in accordance with two DDBD and FBD methodologies in this article. In FBD methodology, the structure seismic design is done based on Iranian Earthquake Resistance Design Code for intermediate ductility class.

Calculations of bending moments and shear forces of beams and columns design for case study designed with DDBD methodology are reported in Tables (1) and (2). Design details of the case study building designed with two methodologies (DDBD based on the model code DBD12 provisions and FBD based on Iranian Earthquake Resistance Design Code provisions) are presented in Table (3). Note that in order to match the DDBD and FBD design methodologies, the design drift limit is considered to be 0.02 in the case study. This value is corresponding to repairable damage limit state in DDBD methodology and life safety limit state in FBD methodology.

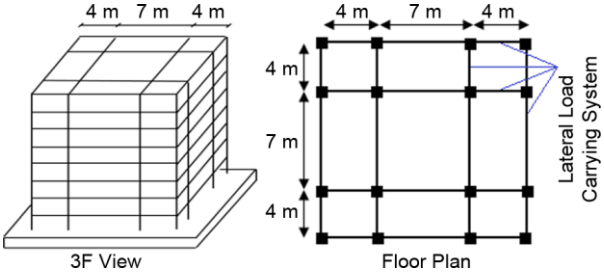

Figure 2. Schematic and plan view of the under-study building.

Table 1. Bending moments and shear forces of beams design for case study designed with DDBD method.

st	$M_{design,\ Outter\ span}$	$M_{design,\ Inner\ span}$	ϕ^0	External Frames		Internal Frames	
				$V_{design,\ Outter\ span}$	$V_{design,\ Inner\ span}$	$V_{design,\ Outter\ span}$	$V_{design,\ Inner\ span}$
8	139.6	145.3	1.25	110.6	93.8	125.7	141.7
7	218.7	229.1	1.25	166.7	125.6	181.5	173.2
6	290.9	304.7	1.25	216.8	154.3	231.7	201.9
5	348.5	367.4	1.25	260	178.8	274.7	226
4	394	418.1	1.25	295.8	199.1	310.3	245.9
3	433.1	459.7	1.25	323.8	215.1	338.2	261.9
2	460.1	488.3	1.25	343.1	226.1	357.5	272.9
1	474.1	503.1	1.25	353.1	231.8	367.5	278.6
							Units:kN, m

Note: In this table, *M* stands for moment, *V* for shear force, and ϕ^0 is overstrength factor.

Table 2. Bending moments and shear forces of columns design for case study designed with DDBD method.

st	μ	ϕ^0	ω_f	$M_{N1,\ Design}$ Exterior Column	$M_{N2,\ Design}$ Interior Column	ϕ_s	$V_{N1,\ Design}$ Exterior Column	$V_{N2,\ Design}$ Interior Column
8	1.03	1.25	1	169.94	339.88	0.75	163.29	326.58
7	1.17	1.25	1.09	183.28	366.56	0.75	246.98	493.96
6	1.47	1.25	1.17	263.17	526.35	0.75	326	651.99
5	1.47	1.25	1.17	319.72	639.44	0.75	387.49	774.97
4	1.47	1.25	1.17	366.63	733.26	0.75	438.5	877
3	1.47	1.25	1.17	403.07	806.14	0.75	478.13	956.26
2	1.47	1.25	1.17	428.2	856.4	0.75	505.46	1010.92
1	1.47	1.25	1.17	441.18	882.37	0.75	519.58	1039.16
								Units:kN, m

Note: In this table, *M* stands for moment, *N* for nominal, *V* for shear force, and μ, ϕ^0, ω_f, and ϕ_s are displacement ductility, overstrength factor, dynamic amplification factor for flexure, and strength reduction factor, respectively.

Table 3. Geometric dimension for prototype building designed with DDBD and FBD methods.

st	Column (Square)			Beam		Column (Square)	Beam	
	Corner Col.	Side Col.	Interior Col.	b_w	h_b		b_w	h_b
8	35	40	40	35	35	35	35	35
7	40	40	40	35	40	40	35	40
6	40	45	45	40	50	40	40	50
5	45	45	45	40	50	45	40	50
4	50	50	50	40	50	50	40	50
3	50	50	50	45	50	50	45	50
2	50	50	50	45	50	50	45	50
1	50	50	50	45	50	50	45	50
	DDBD Design Methodology					FBD Design Methodology		
	NB: b_w is the beam width; h_b is the total beam depth.					Unit: cm		

4. Analytical Modeling

Analytical model is developed in OpenSees framework. For this purpose, beams and columns are modeled using the nonlinear Beam Column element, and sections are considered as Fiber. The behavior model of materials for concrete and steel are concrete02 and steel02, respectively. Also to consider the confinement effect of transverse reinforcements, the parameters of confined concrete are calculated using Mander equations [21].

5. Verification of Modeling

In order to validate the numerical modeling technique used in this study, a two-story RC frame structure tested by Vecchio and Emara [22] is selected. The laboratory structure under-study has been tested using a quasi-static load and it is pushed until collapse occurred. Two constant vertical loads P = 700 kN have been applied at the top of the columns (see Figure 3). In the following, the tested frame geometry has been displayed in Figure 3). As shown in the figure, the frame has a single-span of 3.5 m and the story height of 2 m. The cross-section of columns and beams were reinforced with longitudinal rebars of diameter of 20 mm and stirrups with diameter of 10 mm at 125 mm spacing. The clear cover of beams and columns is 30 and 20 mm, respectively. The material properties i.e., concrete compressive strength, f_c^0, longitudinal rebar yield strength, f_y, and Young's modulus, E_s were considered 30, 418, and 192,500 MPa, respectively.

In Figure (4), the comparability of experimental results [22] with the analytical model developed in OpenSees and other studies results [23-25] has been demonstrated. There is a quite satisfactory agreement between the pushover analysis results of experimental and this study.

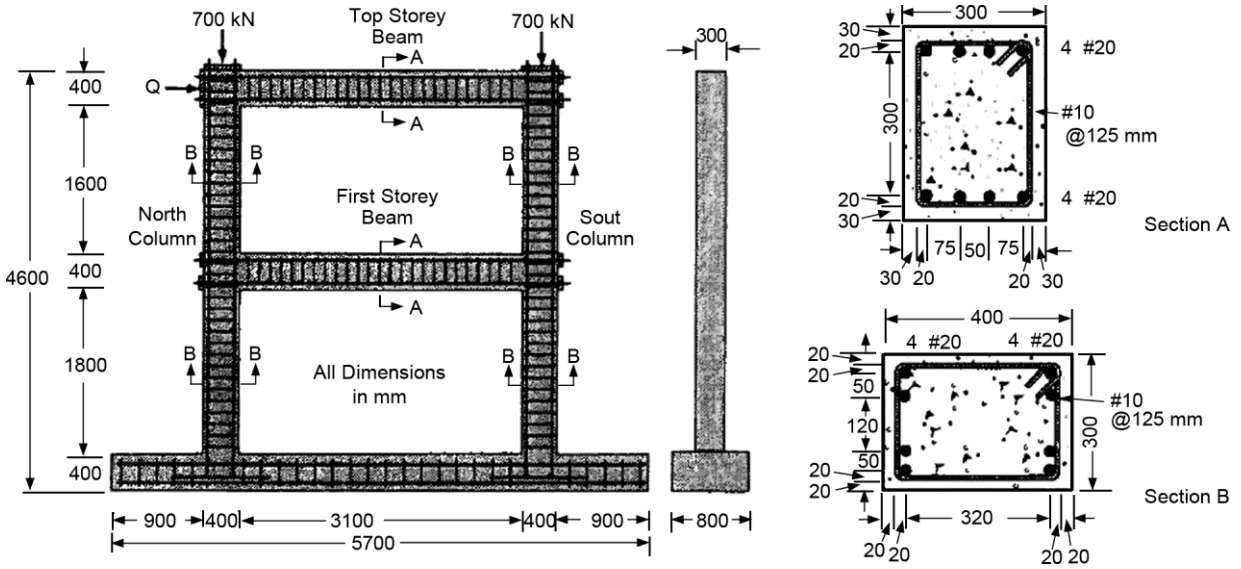

Figure 3. Details of large-scale RC frame tested by Vecchio and Emara [22].

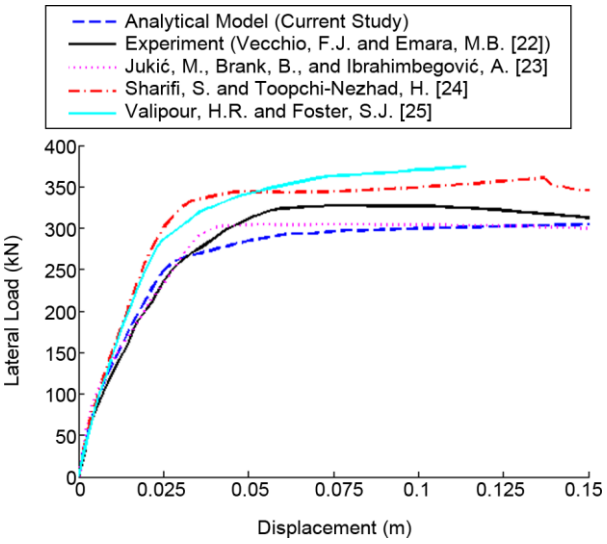

Figure 4. Comparing the results of numerical simulation with experiment.

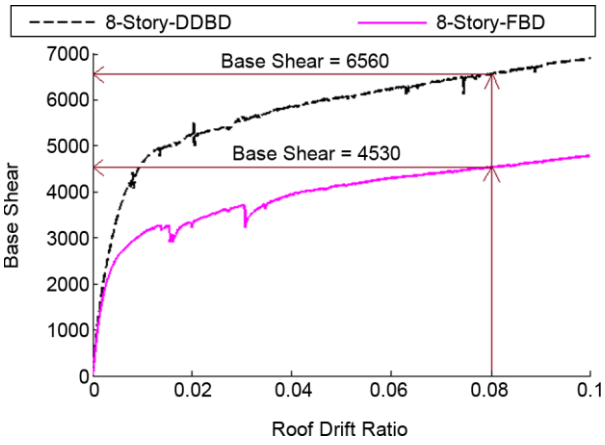

Figure 5. Comparing pushover curves of prototype building designed with DDBD and FBD methodologies.

6. Seismic Response

6.1. Nonlinear Static Analysis of Prototype Building

In the process of performing nonlinear static (pushover) analysis, the procedure presented in FEMA P695 [26] is used. According to provisions of these guidelines, the distribution of forces is performed in accordance with the structure's first-mode under the gravity load combination of 1.05DL + 0.25LL. In nonlinear static analyses, the analysis continues until the center of mass of the structure roof reaches a drift of 10%. In Figure (5), a comparison is made between the pushover curves of 8-story structure designed with two DDBD and FBD methodologies. As can be seen, in a certain amount of drift, e.g. drift of 8%, by changing the design methodology from DDBD to FBD, the base shear is reduced by 45%.

6.2. Nonlinear Dynamic Analysis of Prototype Building

In this article, the Incremental Dynamic Analysis (IDA) is employed to perform the reliability analysis of structures. Due to the dependence of the nonlinear behavior of structures to the earthquake record characteristics (eg frequency content), a set of earthquake records should be used to cover the entire range of structural behavior, i.e., linear to nonlinear.

Table (4) shows specifications of twenty far-field ground motions proposed by FEMA P695. All IDA analyses are done according to Hunt-Fill algorithm [27] and the results are plotted in IM-DM coordinate system. The considered IM (Intensity Measure) and DM (Demand Measure) indices in this study are maximum inter-story drift (θ_{max}) and 5%-damped first mode spectral acceleration ($S_a(T_1, 5\%)$), respectively. In the following, the definition of performance levels i.e., Immediate Occupancy (IO) and Collapse Prevention (CP) are performed according to FEMA-350 [28]. Based on FEMA-350, the IO performance level is defined for θ_{max} of 1.5%, and the CP performance level is defined for θ_{max} of 10% or 20% of the elastic slope. By deriving IDA curves, statistical fractiles are also obtained. There are two methods to draw 16%, 50% and 84% fractiles:

1. IM-based procedure: Based on this procedure, seismic responses (DM) are first sorted from small to large for the specific IM levels, then the numbers of 0.16 n_{rec}, 0.5 n_{rec}, and 0.84 n_{rec} (which for 20 ground motions is 3rd, 10th, and 16th number, respectively) are considered for 16, 50, and 84 percent fractiles, respectively. At low IM values, there is the DM value for all earthquake records, but with the increasing IM, since some records have reached the CP limit state, there is no DM value for those records. Thus, a big number indicating collapse must be considered for those records. Consequently, when seismic responses are sorted from small to large, those large numbers are placed at the bottom of the list. Note that in calculating the fractiles, instead of using the median numbers (i.e., 0.16 n_{rec}, 0.5 n_{rec}, and 0.84 n_{rec}), the mean numbers can also be used. However, because in higher earthquake intensities, a number of earthquake records collapse, calculation of mean numbers is faced with a problem.
2. DM-based procedure: In this procedure, at each level of the damage index (i.e., same DM), the IM values are sorted from small to large, and then the fractiles of 16, 50, and 84% are calculated. The disadvantage of the DM-based procedure is that since IDA curves of some earthquake records have successive segments of hardenings and softenings, there are several responses for an earthquake record at a specific DM level, and this issue makes it difficult to calculate 16, 50, and 84 percent fractiles.

Table 4. List of the considered earthquake records.

No.	Earthquake event	M_w	Station	NEHRP class	PGA/g
GM1	Chi-Chi, 1999	7.6	CHY101	D	0.44
GM2	San Fernando, , 1971	6.6	LA-Hollywood Stor	D	0.21
GM3	Friuli, 1976	6.5	Tolmezzo	C	0.35
GM4	Hector Mine, 1999	7.1	Hector	C	0.34
GM5	Kocaeli, 1999	7.5	Arcelik	C	0.22
GM6	Kocaeli, 1999	7.5	Duzce	D	0.36
GM7	Northridge, 1994	6.7	Canyon Country-WLC	D	0.48
GM8	Northridge, 1994	6.7	Beverly Hills - Mulhol	D	0.52
GM9	Imperial Valley, 1979	6.5	Delta	D	0.35
GM10	Imperial Valley, 1979	6.5	El CentroArray#11	D	0.38
GM11	Landers, 1992	7.3	Yermo Fire Station	D	0.24
GM12	Landers, 1992	7.3	Coolwater	D	0.42
GM13	Loma Prieta, 1989	6.9	Capitola	D	0.53
GM14	Loma Prieta, 1989	6.9	Gilroy Array #3	D	0.56
GM15	Superstition, 1987	6.5	H. El Centro Imp. Co.	D	0.36
GM16	Superstition, 1987	6.5	H. Poe Road (temp)	D	0.45
GM17	Kobe, 1995	6.9	Nishi-Akashi	C	0.51
GM18	Kobe, 1995	6.9	Shin-Osaka	D	0.24
GM19	Manjil, 1990	7.4	Abbar	C	0.51
GM20	Cape Mendo, 1992	7.0	Rio Dell Overpass	D	0.55

In this study, IM-based procedure to draw statistical fractiles has been used. In Figure (6), the IDA curves of the 8-story structure designed with two DDBD and FBD methodologies have been illustrated. As shown, in θmax of 0.06, IM value for 50th percentile (median) curve of the 8-story structure designed with DDBD methodology is reached to a value of 3 g and for the 8-story structure designed with FBD methodology is reached to a value of 1 g. Consequently, this significant reduction in the damage index indicates the inadequacy of FBD design methodology.

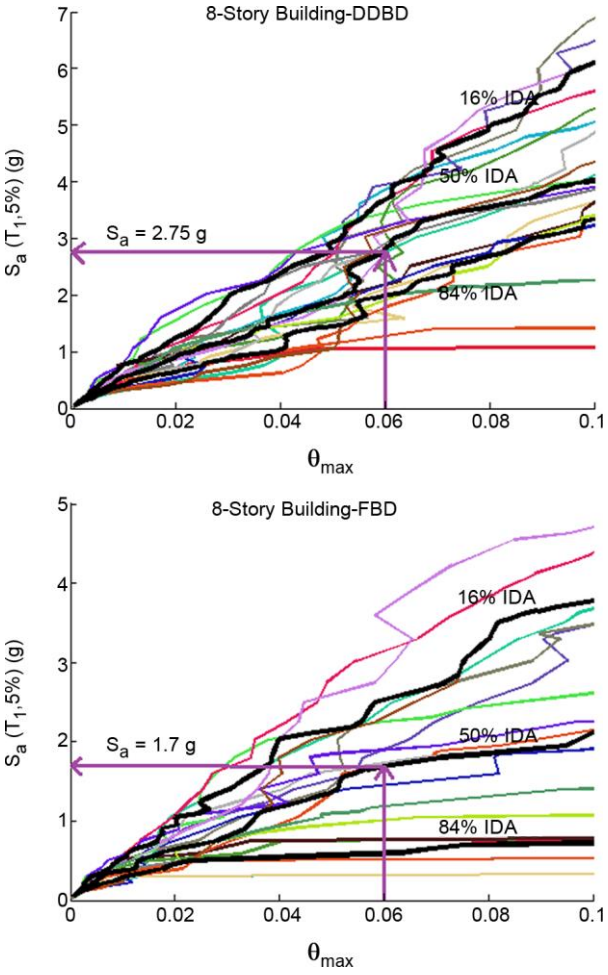

Figure 6. IDA curves of prototype building designed with DDBD and FBD methodologies.

7. Reliability Theory Formulation

In this study, the reliability assessment of structure designed with DDBD and FBD methodologies is performed with the aim of estimating confidence level and calculating MAF of exceedance. The following approximations [29] are used to calculate the MAF:

- It is assumed that the hazard curve can be expressed exponentially near the desired performance level in accordance with the following equation:

$$H(S_a) = k_0 S_a^{-k} \quad (1)$$

Parameters k and k_0 are coefficients for linear regression of hazard.

- It is assumed that the drift demand can be approximated by the following equation:

$$\hat{D} = a(S_a)^b \quad (2)$$

where a and b are regression coefficients for linear regression.

- It is assumed that the drift demand curve is log-normal and has a standard deviation equal to $\beta_{D/Sa}$ (dispersion factor).

7.1. Calculation of MAF

The MAF can be determined based on two evaluation procedures of "appraisal by considering the only source of uncertainty" and "appraisal by considering randomness and uncertainty as the sources of uncertainty" [17].

7.1.1. Appraisal by Considering the Only Source of Uncertainty

In calculating MAF, when only the aleatory uncertainty is contemplated for estimating the median of drift demand and drift capacity, the value of this parameter is obtained from Equation (3). Note that IDA analysis results are used to calculate drift demand median and drift capacity median.

$$P_{PL} = H(\hat{S_a^c}) \exp[\frac{1}{2}\frac{k^2}{b^2}(\beta^2_{D/S_a} + \beta^2_C)] \quad (3)$$

where:

$$H(\hat{S_a^c}) = k_0(\hat{S_a^c})^{-k} \quad (4)$$

in which, S_{ac} is the spectral acceleration of drift capacity level, $\beta_{D/Sa}$ is dispersion measure for drift demand and βc is dispersion measure for drift capacity.

7.1.2. Appraisal by Considering the Only Source of Uncertainty

In calculating MAF, when uncertainties of aleatory and epistemic are contemplated for estimating the median of drift demand and drift capacity, the value of this parameter is obtained from Equation (5):

$$P_{PL} = H(S_a^{\hat{c}}) \exp[\frac{1}{2}\frac{k^2}{b^2}(\beta_{D/S_a}^2 + \beta_{UD}^2)] \times \exp[\frac{1}{2}\frac{k^2}{b^2}(\beta_C^2 + \beta_{UC}^2)] \quad (5)$$

where:

$$H(S_a^{\hat{c}}) = k_0 (S_a^{\hat{c}})^{-k} . \exp(\frac{1}{2}\beta_{UH}^2) \quad (6)$$

$$\beta_{UD} = \frac{\beta_{D/S_a}}{\sqrt{n_{rec}}} \quad (7)$$

in which, β_{UD} is demand uncertainty, β_{UC} is capacity uncertainty and is assumed to be 0.2 for 8-story structure, β_{UH} is assumed to be 0.5 in this study, and n_{rec} is the number of earthquake records.

7.2. Calculation of Confidence Level

The calculating confidence level of structure is performed from:

$$CL = \varphi(K_x) \quad (8)$$

where:

$$K_x = -\frac{1}{\beta_{UT}} Ln(\frac{\gamma.D}{\varphi.C}) \quad (9)$$

in which, K_x is standardized Gaussian variate, β_{UT} is total uncertainty and for the case study building equal to 0.2 at IO performance level and equal to 0.425 at CP performance level is considered according to FEMA-350, and γ_D and ϕ_C are factored demand and factored capacity, respectively. The value of parameters of γ and ϕ can be calculated based on Equation (10) and Equation (11), respectively.

$$\gamma = \exp[\frac{1}{2}\frac{k}{b}\beta_{D/S_a}^2] \quad (10)$$

$$\varphi = \exp[-\frac{1}{2}\frac{k}{b}\beta_C^2] \quad (11)$$

8. Investigation of Results of Reliability Analysis

8.1. Investigation of Effect of Two Probabilistic Procedures on MAF Estimation

In Table (5), the MAF of exceeding the IO and CP performance levels has been illustrated. As seen, by changing the evaluation procedure from "appraisal by considering the only source of uncertainty" to "appraisal by considering randomness and uncertainty as the sources of uncertainty", the MAF value of exceeding the IO and CP performance levels for DDBD methodology is changed from 3.61×10^{-4} to 4.47×10^{-4} and 2.41×10^{-5} to 3.01×10^{-5}, respectively. Whereas for FBD methodology, it is changed from 6.35×10^{-4} to 7.7×10^{-4} and 5.58×10^{-4} to 6.89×10^{-4}, respectively. Hence, based on the results, it can be said that by considering aleatory and epistemic uncertainties, the MAF increases above 20 to 25 percent. Increasing this parameter increases the vulnerability of the structure. In comparing DDBD and FBD methodologies, the MAF value of exceeding the IO and CP performance levels under both aleatory and epistemic uncertainties for DDBD methodology are reached 3.61×10^{-4} and 2.41×10^{-5} and for FBD

Table 5. Comparing MAF of exceeding limit state by different probabilistic procedures.

	DDBD-The Only Source of Uncertainty		DDBD-Randomness and Uncertainty as the Sources of Uncertainty	
	IO	**CP**	**IO**	**CP**
MAF	3.61E-04	2.41E-05	4.47E-04	3.01E-05

	FBD-The Only Source of Uncertainty		FBD-Randomness and Uncertainty as the Sources of Uncertainty	
	IO	**CP**	**IO**	**CP**
MAF	6.35E-04	5.58E-04	7.70E-04	6.89E-04

methodology are reached 6.35×10^{-4} and 5.58×10^{-4}. As a result, it can be stated that by moving from FBD to DDBD methodology, MAF of exceeding the IO and CP performance levels decreases significantly.

8.2. Investigation of Confidence Level Changes vs. Drift Demand and Earthquake Intensity for Two DDBD and FBD Design Methodologies

The effect of seismic design methodologies on the structural confidence level has been investigated in Figure (7). A quick look at curves represented in Figure (7a) depicts that the structure designed with DDBD, unlike FBD methodology, up to the 4 g spectral acceleration satisfies 35% confidence level. In other words, FBD-designed structure at the spectral acceleration value of 2 g reaches to 0% confidence level. In the following, based on the mentioned figure, the spectral acceleration corresponding to 25, 50, 75, and 100% confidence levels for both DDBD and FBD methodologies can be derived. The results have been reported in Table (6). It is observed that the spectral acceleration at the 75% confidence level for DDBD-designed structure is 2.54 g whereas for FBD-designed structure is 0.52 g. Also, at 25% confidence level, the spectral acceleration value for the prototype structure designed with DDBD and FBD methodologies is equal to 4.53 and 0.88 g, respectively. Hence, it can be said that the spectral acceleration decreases dramatically by moving from the DDBD to FBD methodology for a specific value of confidence level. Finally, the decrease rate of structure confidence levels with demand increasing from 0 to 0.15 has been revealed in Figure (7b). In the structure designed with FBD methodology, the confidence level reaches zero at a demand value of 0.05. Whereas for the structure designed with DDBD methodology, a 79% confidence level is provided at the same value of demand and it is observed that the confidence level of 50% is still provided at the demand value of 0.071. This subject shows the great performance of DDBD methodology in the seismic design of structures.

8.3. Investigation of Effect of Using Two Design Methodologies in Distribution of Drift Demand and Confidence Level

In Figure (8a), the diagram of seismic demand changes under hazard levels of SLE25, SLE43, SLE72, DBE, MCE, and OVE has been displayed. By having seismic demand corresponding to hazard levels of low to high, confidence levels

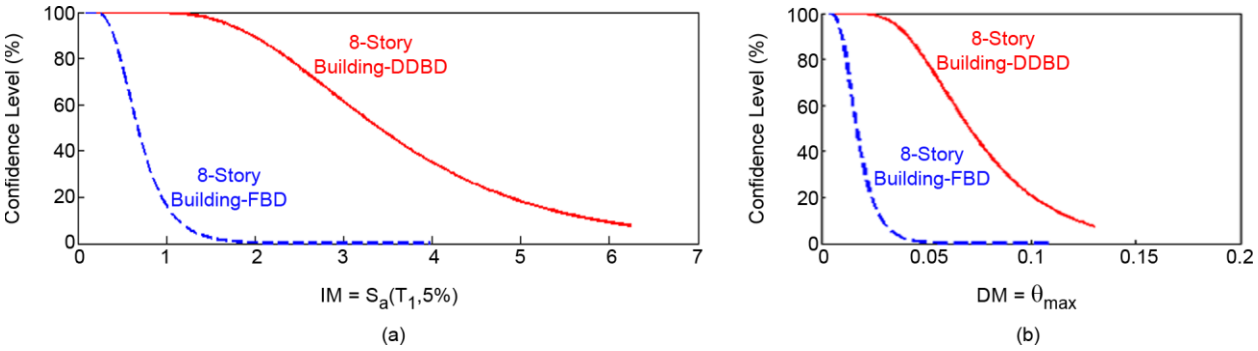

Figure 7. Curve of confidence level changes against a. seismic demand and b. seismic intensity.

Table 6. Calculation of spectral acceleration corresponding to 25, 50, 75, 100% confidence levels for DDBD and FBD methodology.

Spectral Acceleration Corresponding to a Confidence Level of 100%		Spectral Acceleration Corresponding to a Confidence Level Of 75%	
DDBD	**FBD**	**DDBD**	**FBD**
1.02 g	0.22 g	2.54 g	0.52 g
Spectral Acceleration Corresponding to a Confidence Level of 50%		**Spectral Acceleration Corresponding to a Confidence level of 25%**	
DDBD	**FBD**	**DDBD**	**FBD**
3.39 g	0.67 g	4.53 g	0.88 g

versus these hazard levels are obtained (see Figure 8b). These six hazard levels namely SLE25, SLE43, SLE72, DBE, MCE, and OVE have return periods of 25, 43, 72, 475, 2475, and 4975 years, respectively. As seen in Figure (8-a), by moving from the hazard level of SLE25 to OVE, the maximum demand value with a steep upward slope increases, and eventually, it reaches its maximum value at the OVE hazard level. For example, the maximum demand value at SLE25 hazard level corresponding to the CP performance level for the structure designed with DDBD methodology is equal to 0.0019, and it is reached to 0.025 for OVE hazard level corresponding to the CP performance level. Checking the confidence levels of structure designed with both DDBD and FBD methodologies at hazard levels of SLE25 to DBE corresponding to IO and CP performance levels (Figure 8-b) shows that it is reached to 95-99% because earthquakes with the return periods from 25 to 72 years are not among the strong earthquakes. Whereas at MCE and OVE hazard levels, the conditions for both mentioned design methodologies are quite different. For instance, at IO performance level corresponding to MCE and OVE hazard levels, DDBD-designed structure achieves 61 and 8% confidence level, respectively, and the confidence level of 99% is provided at CP performance level.

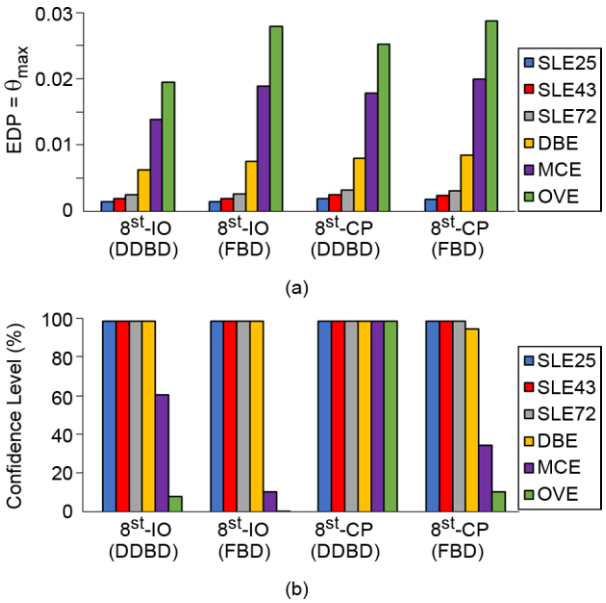

Figure 8. Distribution of (a) drift demand and (b) confidence level at different hazard levels for the DDBD and FBD methodologies.

However, by changing the design methodology from DDBD to FBD, the confidence levels versus MCE and OVE hazard levels at both IO and CP performance levels reduce. Hence, it can be said that reliability reduces dramatically by moving from DDBD to FBD.

9. Conclusion

Based on the probabilistic seismic performance appraisal of the 8-story RC frame building designed with DDBD and FBD methodologies, the following conclusions are obtained:

- The results of nonlinear evaluations showed that both pushover and IDA curves of structure designed with DDBD methodology, which derived from nonlinear analyses, are placed at a higher level than the curves of structure designed with FBD methodology. In other words, for a certain amount of roof drift, the base shear in the pushover curve of DDBD-designed structure increases dramatically compared to the pushover curve of FBD-designed structure. Besides, in IDA median curve, the earthquake intensity decreases dramatically for a certain amount of inter-story drift by moving from the DDBD to FBD methodology.
- In checking the vulnerability of the structure under study, it was concluded that by applying both aleatory and epistemic uncertainties, the MAF value of exceeding the immediate occupancy and collapse prevention increases in comparability to the state where only aleatory uncertainty is contemplated.
- The MAF value of exceedance considerably increases by changing the methodology from DDBD to FBD. The increasing this parameter indicates that the overall probability of failure in FBD-designed structure has increased.
- In investigating the confidence level changes versus intensity and demand, it was observed that by moving the design methodology from FBD to DDBD, the confidence level signify-cantly increases for a specific value of demand and intensity.
- By calculating the confidence level at different levels of seismic hazard, it was observed that

the structure designed with DDDB methodology, in contrast to FBD methodology is safe and provides the 99% confidence level at severe seismic hazard levels against the CP performance level.

References

1. Priestley, M.J.N. and Kowalsky, M.J. (2000) Direct displacement-based seismic design of concrete buildings. *Bulletin of the New Zealand Society for Earthquake Engineering*, **33**(4), 421-441.

2. Pettinga, J.D. and Priestley, M.J.N. (2005) Dynamic behaviour of reinforced concrete frames designed with direct displacement-based design. *Journal of Earthquake Engineering*, **9**(SPEC. ISS. 2), 309-330.

3. Rahman, M.A. and Sritharan, S. (2006) An evaluation of force-based design vs. direct displacement-based design of jointed precast post-tensioned wall systems. *Earthquake Engineering and Engineering Vibration*, **5**(2), 285-296.

4. Sullivan, T.J. (2011) Direct displacement-based design of a RC wall-steel EBF dual system with added dampers. *Bulletin of the New Zealand Society for Earthquake Engineering*, **44**(3), 167-178.

5. Malekpour, S., Ghaffarzadeh, H., and Dashti, F. (2011) Direct displacement based design of regular steel moment resisting frames. *Procedia Engineering*, **14**, 3354-3361.

6. Sullivan, T., Maley, T., and Calvi, G.M. (2011) Seismic response of steel moment resisting frames designed using a Direct DBD procedure. *Proceedings of the 8th International Conference on Structural Dynamics, EURODYN*.

7. Wijesundara, K. and Rajeev, P. (2012) Direct displacement-based seismic design of steel concentric braced frame structures. *Australian Journal of Structural Engineering*, **13**(3),243-257.

8. Sullivan, T.J., Bono, F., Magni, F., and Calvi, G.M. (2012) Development of a computer program for direct displacement-based design. *15th World Conference Earthquake Engineering*.

9. Priestley, M.J.N., Calvi, G.M., and Kowalsky, M. (2007) *Displacement-Based Seismic Damage of Structures*. Pavia, Italy: IUSS Press.

10. Sullivan, T.J., Priestley, M.J.N., and Calvi, G.M. (2012) *A Model Code for the Displacement-Based Seismic Design of Structures DBD12*.

11. Nievas, C.I. and Sullivan, T.J. (2014) Developing the direct displacement-based design method for RC strong frame-weak wall structures. *Second European Conference on Earthquake Engineering and Seismology*, Instanbul 25-29.

12. Salawdeh, S. and Goggins, J. (2016) Direct displacement based seismic design for single storey steel concentrically braced frames. *Earthquake and Structure*s, **10**(5), 1125-1141.

13. Peng, C. and Guner, S. (2018) Direct displacement-based seismic assessment of concrete frames. *Computers and Concrete*, **21**(4), 355-365.

14. Ye, K., Xiao, Y., and Hu, L. (2019) A direct displacement-based design procedure for base-isolated building structures with lead rubber bearings (LRBs). *Engineering Structures*, **197**, 109402.

15. Sharma, A., Tripathi, R.K., and Bhat, G. (2020) Comparative performance evaluation of RC frame structures using direct displacement-based design method and force-based design method. *Asian Journal of Civil Engineering*, **21**(3), 381-394.

16. Senthilkumar, R. and Satish Kumar, S.R. (2020) Seismic performance of semi-rigid steel-concrete composite frames. *Structures*, **24**, 526-541.

17. Jalayer, F. and Cornell, C.A. (2003) *A Technical Framework for Probability-Based*

Demand and Capacity Factor Design (DCFD) Seismic Formats. Report No. 2003/08, Pacific Earthquake Engineering Center, Berkeley, CA.

18. Priestley, M.J.N., Calvi, G.M., and Kowalsky, M.J. (2007) Direct displacement-based seismic design of structures. *NZSEE Conference*

19. Shibata, A. and Sozen, M.A. (1976) Substitute-structure method for seismic design in R/C. *Journal of the Structural Division*, **102**(1), 1-18.

20. Standard No. 2800 (2015) *4th Edition of Iranian Code of Practice for Seismic Resistance Design of Buildings*. Building and Housing Research Center, Iran (in Persian).

21. Mander, J.B., Priestley, M.J.N., and Park, R. (1988) Theoretical stress-strain model for confined concrete. *Journal of Structural Engineering*, **114**(8), 1804-1826.

22. Vecchio, F.J. and Emara, M.B. (1992) Shear deformations in reinforced concrete frames. *ACI Structural Journal*, **89**(1), 46-56.

23. Jukić, M., Brank, B., and Ibrahimbegović, A. (2013) Embedded discontinuity finite element formulation for failure analysis of planar reinforced concrete beams and frames. *Engineering Structures*, **50**, 115-125.

24. Sharifi, S. and Toopchi-Nezhad, H. (2018) Seismic response modification factor of RC-frame structures based on limit state design. *International Journal of Civil Engineering*, **16**(9), 1185-1200.

25. Valipour, H.R. and Foster, S.J. (2010) A total secant flexibility-based formulation for frame elements with physical and geometrical nonlinearities. *Finite Elements in Analysis and Design*, **46**(3), 288-297.

26. Federal Emergency Management Agency (2009) *Quantification of Building Seismic Performance Factors*. Washington, DC: FEMA P695.

27. Vamvatsikos, D. (2011) Performing incremental dynamic analysis in parallel. *Computers and Structures*, **89**(1-2), 170-180.

28. Federal Emergency Management Agency (2000) *Recommended Seismic Design Criteria for New Steel Moment-Frame Buildings*. Washington, D.C: FEMA-350.

29. Cornell, C.A., Jalayer, F., Hamburger, R.O., and Foutch, D.A. (2002) Probabilistic basis for 2000 SAC federal emergency management agency steel moment frame guidelines. *Journal of Structural Engineering*, **128**(4), 526-533.